J Nanopart Res (2010) 12:1401–1414
DOI 10.1007/s11051-009-9686-y

RESEARCH PAPER

# Room temperature synthesis of an optically and thermally responsive hybrid PNIPAM–gold nanoparticle

**J. Ruben Morones · Wolfgang Frey**

Received: 23 March 2009 / Accepted: 23 June 2009 / Published online: 21 July 2009


**Abstract** Composites of metal nanoparticles and environmentally sensitive polymers are useful as nano-actuators that can be triggered externally using light of a particular wavelength. We demonstrate a synthesis route that is easier than grafting techniques and allows for the in situ formation of individual gold nanoparticles encapsulated by an environmentally sensitive polymer, while also providing a strong interaction between the polymer and the metal particle. We present a one-pot, room-temperature synthesis route for gold metal nanoparticles that uses poly-*N*-isopropyl acrylamide as the capping and stabilizing agent and ascorbic acid as the reducing agent and achieves size control similar to the most common citric acid synthesis. We show that the composite can be precipitated reversibly by temperature or light using the non-radiative decay and conversion to heat of the surface plasmon resonance of the metal nanoparticle. The precipitation is induced by the collapse of the polymer cocoon surrounding each gold nanoparticle, as can be seen by surface plasmon spectroscopy. The experiments agree with theoretical models for the heat generation in a colloidal suspension that support fast switching with low laser power densities. The synthesized composite is a simple nanosized opto-thermal switch.

**Keywords** Gold nanoparticles · *N*-isopropyl acrylamide (PNIPAM) · Surface plasmons · Ascorbic acid · Environmentally responsive polymers · Optical switch · Heat conduction

**Electronic supplementary material** The online version of this article (doi:10.1007/s11051-009-9686-y) contains supplementary material, which is available to authorized users.

W. Frey (✉)
Department of Biomedical Engineering, The University of Texas at Austin, 1 University Station, C0800, Austin, TX 78712, USA
e-mail: wfrey@mail.utexas.edu

W. Frey
Center for Nano and Molecular Science and Technology, The University of Texas at Austin, Austin, TX 78712, USA

J. R. Morones
Department of Chemical Engineering, The University of Texas at Austin, 1 University Station, C0400, Austin, TX 78712, USA
e-mail: morones@bu.edu

*Present Address:*
J. R. Morones
Department of Biomedical Engineering, Boston University, Boston, MA, USA

J. R. Morones
Howard Hughes Medical Institute, Boston University, Boston, MA, USA

## Introduction

Nanoswitches that provide a mechanical response to a localized trigger are important for sensing purposes,

(Ben-Moshe et al. 2006; Calvert 2008; Hilt et al. 2006) for biotechnological applications such as the control of microfluidic flow or enzyme activity, and for modifying surface properties upon an external trigger (Beebe et al. 2000; Eddington and Beebe 2004; Frey et al. 2003a; Kaholek et al. 2004; Lahann and Langer 2005; Sershen et al. 2005; Shimoboji et al. 2002; Yousaf et al. 2001). Mechanical actuation can come from advanced functional nanomaterials that respond to changes in their local environment by performing a conformational transition (Calvert 2008; Gil and Hudson 2004; Jager et al. 2000; Jiang et al. 2006; Peppas et al. 2006). Such conformational changes can be triggered by varying the chemical composition or the thermodynamic conditions around the material. Chemical triggers include changes in the pH (Dai et al. 2008; Eddington and Beebe 2004; Peppas and Khare 1993) or, more generally, the presence of a specific molecule (Byrne et al. 2002; Liu and Lu 2006; Schild 1992). Thermodynamic changes include temperature (Frey et al. 2003b; Nath and Chilkoti 2001; Schild 1992), pressure (Juodkazis et al. 2000), an externally applied voltage (Shoenfeld and Grodzinsky 1980; Zheng et al. 2008), and exposure to light (Irie and Kungwatchakun 1992; Jiang et al. 2006; Kungwatchakun and Irie 1988; Nayak and Lyon 2004; Radt et al. 2004; Slocik et al. 2007; Szilagyi et al. 2007).

While most research has used temperature or pH to trigger a conformational change in polymers or gels, optically responsive materials are particularly interesting because the stimulus, light, can be applied highly localized and without direct contact with the switch. Typical processes used for optical switching are conformational changes of dye molecules, such as azobenzene or spiropyrane derivatives, integrated into the polymer backbone or as pendent groups (Edahiro et al. 2005; Garcia et al. 2007; Higuchi et al. 2004; Jiang et al. 2006; Nayak et al. 2006; Zhu et al. 2007), or the local generation of heat due to dyes or metal nanoparticles, which are either covalently linked or simply trapped in a thermally responsive polymer or peptide hydrogel (Nayak and Lyon 2004; Owens et al. 2007; Sershen et al. 2002; Slocik et al. 2007; Strzegowski et al. 1994). While dye molecules have the advantage of allowing switching in both directions, the dyes are chemically reactive and susceptible to bleaching, and the switching process is slow (Brinker 2004; Hugel et al. 2002; Kungwatchakun and Irie 1988; Shimoboji et al. 2002). Although metal nanoparticles cannot induce switching in both directions, they have the advantage that the particles are very stable. The generated heat dissipates quickly in most environments so that the cooling process can provide a passive reverse response mechanism once the trigger is turned off. Gold nanoparticles, in particular, are inert and biocompatible (Langer and Tirrell 2004), and therefore have been used in drug delivery systems to optically actuate hydrogel–metal nanoshells (Sershen et al. 2000) for therapeutic ablation, (O'Neal et al. 2004) and as responsive valves in microfluidic devices (Eddington and Beebe 2004; Sershen et al. 2005).

The combination of a thermally responsive polymer or hydrogel and metal nanoparticles creates an optically switchable nanocomposite by converting light into heat through the non-radiative decay of surface plasmon resonances (Hutter and Fendler 2004), and hence inducing the collapse of the polymer. Since it is the non-radiative part of the extinction that is used for heat production and thus for the switching mechanism, the material, shape, and size of the metal nanoparticles have to be optimized for efficient heat generation and to match the wavelength range desired (Halas 2005; Jain et al. 2006; Liz-Marzan 2006). Often poly-*N*-isopropyl acrylamide (PNIPAM), one of the most studied non-toxic environmentally responsive polymers, is chosen as the thermally responsive polymer surrounding the metal nanoparticle. PNIPAM has a lower critical solution temperature (LCST) of around 32 °C in water (Schild 1992), which makes it attractive for biological applications (Hoffman and Stayton 2004).

Combining PNIPAM and gold nanoparticles has been achieved through physical entrapment, such as polymerizing a PNIPAM gel around previously formed nanoparticles (Sershen et al. 2005; Sershen et al. 2002; Sershen et al. 2001), by chemical grafting of PNIPAM to prefabricated gold nanoparticles, and by in situ synthesis of gold nanoparticles in the presence of functional groups on linear polymers or crosslinkers. Grafting techniques truly couple the PNIPAM to the particle surface (Liu and Lu 2006), and grafting to (Xu et al. 2007; Zhu et al. 2004) and from (Kim et al. 2005; Pyun et al. 2003; Raula et al. 2003) existing gold nanoparticles using surface-initiated polymerization has been demonstrated.

Grafting to and from existing gold nanoparticles has the advantage that the size can be chosen freely, but the initial stabilizing agent must be chemically modified or exchanged (Kim et al. 2005; Nuss et al. 2001). However, thiols, dithiols, and thioesters can act as capping and stabilizing agents in the synthesis of gold clusters (Brust et al. 1995; Brust et al. 1994; Raula et al. 2003), and therefore thiol-containing initiators in atom-transfer radical polymerization (ATRP) (Ohno et al. 2002) and the dithioester end group of reversible addition/fragmentation chain transfer (RAFT) pre-polymerized polymers (Shan et al. 2003; Shan et al. 2005) can be used directly for the gold nanoparticle synthesis, although the resulting particle size is typically relatively small. In gels, in situ reduction of gold has been achieved in the presence of PNIPAM using thiol-based cross-linkers (Pong et al. 2006; Wang et al. 2004) or by using the prefabricated PNIPAM hydrogel (Kim and Lee 2007) Both techniques produce gold nanoparticles with relatively broad absorption spectra, indicating broad particle size distributions and low growth control. Moreover, using thiol-containing cross-linkers couples the mechanical properties of the gel to the growth of the metal nanoparticles.

So far, optically responsive actuators controlled by non-radiative heat dissipation of optical resonances in metal nanoparticles have been demonstrated only for hydrogel composites which typically have long response times induced by the cross-links, and often require high-power lasers to trigger the response (Nayak and Lyon 2004; Sershen et al. 2002) Polymer-nanoparticle composites, which lack cross-links and allow for an aggregation of nanoparticles without significant interpenetration of the polymers, will lead to much faster switching behavior with lower power lasers. The heat generated in the gold nanoparticle is transferred to the polymer shell within picoseconds (Ge et al. 2005).

Here, we present a synthesis route that creates gold–PNIPAM composites with individual PNIPAM molecules acting in two roles: as a capping and stabilizing agent in the gold synthesis, and as trigger to optically reduce the solubility of the gold–PNIPAM composite, and induce aggregation that is reversible upon turning off the light. The PNIPAM is linked to the gold through the synthesis, but, unlike RAFT–PNIPAM-synthesized composites achieves far larger nanoparticles, which are needed for efficient conversion of light to heat. The ascorbic acid (AsA)-based one-pot synthesis strategy achieves good size control without the need to first create gold seeds with a strong reducing agent. The PNIPAM–gold composite particles produced here are approximately 30 nm in size and are thermally and optically responsive using a convenient 532 nm laser line. The reversible aggregation upon external thermal or optical stimulus leads to a small shift in the localized surface plasmon resonance (LSPR) peak in the extinction spectrum. We compare the experimental data to analytical and numerical models for the kinetics and steady state of the optically and thermally driven aggregation and show that fast response times in both directions can be achieved with relatively low laser power.

## Results and discussion

### Synthesis of colloidal gold nanoparticles

Experiments using various ratios of $NaBH_4$ to Au show that $NaBH_4$ is too strong for a controlled gold acid reduction and produces only very small nanoparticles (<10 nm). This is in contrast to gold reduction in the presence of NIPAM-PEG-PVP triblock-copolymers (Zheng et al. 2006) and the reduction of silver, (Morones and Frey 2007) but agrees with the use of $NaBH_4$ to produce very small nanoparticles or gold seeds using other capping agents (Ballauff and Lu 2007; Brown et al. 2000) Small particles will lead to very low light absorption and insufficient energy conversion to create the heat needed for optical switching (Jain et al. 2006). Conventional sodium citrate reduction uses high temperatures, which are incompatible with hydrated PNIPAM, and narrow size distributions of spherical particles with diameters >40 nm are difficult to obtain (Frens 1973; Jana et al. 2001a, b; Niu et al. 2007) The far milder reducing agent AsA can produce narrow size distributions of larger gold particles, but typically requires a seeding step using $NaBH_4$ followed by several growth steps to fabricate spheres (Brown et al. 2000; Jana et al. 2001b; Kimling et al. 2006) and rods (Shiotani et al. 2007). So far, AsA reduction without initial $NaBH_4$ seeds has produced large agglomerated particles with broad shape and size distributions for a variety of capping agents (Goia and Matijevic 1998, 1999; Jana et al.

2001a; Kimling et al. 2006) The only exception, resulting in the successful use of AsA to stabilize gold seeds was at very low ionic gold concentrations, two orders of magnitude lower than the concentrations reported here (Andreescu et al. 2006).

We found that PNIPAM allows us to use AsA as the reducing agent in four identical synthesis steps, rather than a nucleation or seeding step using a strong reducing agent and consecutive growth steps with AsA. Following an approach similar to the one developed for silver, (Morones and Frey 2007) the acid $HAuCl_4$ is reduced in the presence of a separately polymerized PNIPAM (MW = 510,000). Because PNIPAM is temperature sensitive, the synthesis needs to be performed below the LCST, so that the polymer is hydrated and able to nucleate and stabilize the particles. PNIPAM is dissolved in a dilute gold acid solution at a given molar PNIPAM (repeat units) to gold (ions) ratio (PGR) and allowed to equilibrate for 20 min. Results were compared to a control synthesis consisting of a gold solution reduced without PNIPAM.

The samples after the initial growth step appear as a pale pink suspension indicating the formation of very small metal particles, except for the control, which appears pale blue and within a couple of hours totally loses coloration while large precipitates appear. Three additional growth steps, each time adding molar amounts of ionic gold and AsA as in the first step, lead to a successively stronger wine-red color for all PGRs, while hastening the precipitation in the control. We tested whether the rate at which the reducing agent is added affected the homogeneity of the particle size by adding smaller amounts of reducing agent and gold ions in a larger number of synthesis steps, but found no difference (not shown). A process of preferential reduction of the gold acid at the particle surface, which promotes growth rather than new nucleation and which can achieve large metal particles, has been suggested for AsA (Brown et al. 2000; Jana et al. 2001b).

For silver, the polymer-to-metal molar ratio had a strong influence on the size distribution of the metal particles produced and on the encapsulation by the polymer. In contrast, for gold, the average particle size is nearly PGR-independent, indicating that the PNIPAM is not acting as a nucleating agent. Figure 1 shows representative examples of particles grown for PGRs 360:1 and 20:1. The samples mostly show spherical morphology for PGRs above 45:1, although some triangular shapes can also be found in each case. A detailed analysis of the shapes of the ~200 analyzed particles per PGR showed a circularity index of >0.9 for all PGRs, with less than 5% non-spherical particles for PGRs 180 and 360 (see supplemental information) The higher PGRs (360:1 and 180:1) also show tighter size control with a standard deviation of ~22%, which is similar to both that obtained for sodium citrate (Brown et al. 2000) and that obtained with sodium borohydrate-created seeds using AsA to form particles >20 nm in diameter (Jana et al. 2001b). Lower PGRs show higher standard deviations of ~35%. This shows that the addition of PNIPAM acts as a capping agent and allows a more homogenous growth of the gold particles during the reduction. The interaction of PNIPAM with gold is considered weaker than with silver (Zhao and Crooks 1999), and it can be expected that this plays a more important role at lower capping agent concentrations.

Figure 2 shows a representative negative-stain TEM image of PNIPAM-coated gold nanoparticles in a cocoon-like nanocomposite. Although free PNIPAM can be seen in this image, as described below, it is not responsible for the precipitation by temperature and light; this is similar to the cocoon-like structures that have been observed for silver reduced in the presence of PNIPAM (Morones and Frey 2007). However, unlike for silver, the gold cocoons do not contain multiple particles even at high PGRs, most likely due to Ostwald ripening (see also "Optical characterization of the colloidal gold solution" section).

PNIPAM polymers with thiol- or thioester functionality have been used before as a nucleation center for synthesizing gold nanoparticles at room temperature (Brust et al. 1994; Raula et al. 2003; Shan et al. 2003). PNIPAM gels without thiol functionality have also been used successfully, where the amide group of the NIPAM is assumed to help facilitate the reduction of the gold ions by the AsA (Kim and Lee 2007). Our method of synthesizing PNIPAM–gold nanoparticles is, to the best of our knowledge, the first time that individual linear PNIPAM chains without thiol-type groups have been used successfully to cap and stabilize gold nanoparticles. It was previously attempted without success (Chen et al. 2002), presumably because the interaction of the gold with PNIPAM is weaker than for other metals such as silver (Chen et al. 1998) or platinum Chen and

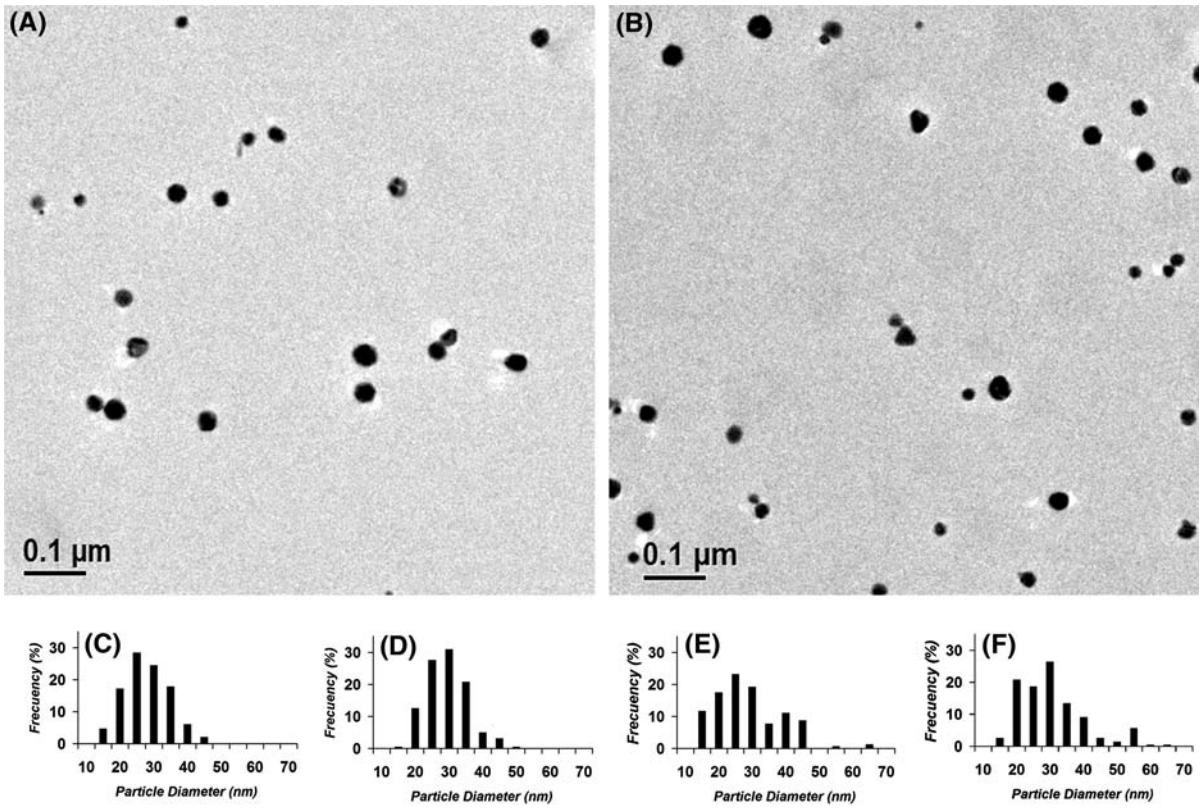


**Fig. 1** Representative TEM images of the PNIPAM–gold nanoparticle composites for PGRs **a** 360:1 and **b** 20:1. Size distributions of about 200 particles each chosen randomly from different areas of the carbon grid for PGRs **c** 360:1, **d** 180:1, **e** 45:1, and **f** 20:1. Higher PGRs allow good size control

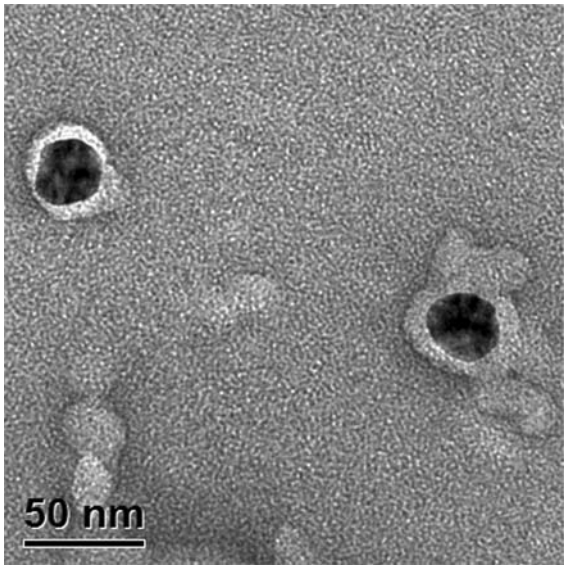


**Fig. 2** TEM image of the PGR 360:1 sample negatively stained with uranyl acetate. The particles are entrapped in polymer shells

Akashi 1997). Two additional factors may have contributed to the broad size distribution in that case: a synthesis temperature above the LCST, and the simultaneous polymerization of PNIPAM grafts and the reduction of the Au ions with the initiator and the free radicals formed during the polymerization. Individual polymer chains of a PNIPAM–PEG–PVP triblock-copolymer have been used to synthesize gold nanoparticles of defined size, but here a hydrophobic core was important in the synthesis (Zheng et al. 2006).

The presumed weaker interaction between pure PNIPAM and gold could, however, allow for the growth of larger gold nanoparticles compared to those produced by stronger thiol-based stabilization polymers, as indicated by the influence of PNIPAM polydispserity on the size distribution of the gold core (Shan et al. 2003). Still, our synthesis route, which does not rely on thiol-type gold binding groups, provides for a strong enough interaction between

polymer and gold nanoparticle, as indicated by the composite remaining intact through repeated precipitation-solubilization cycles, as demonstrated below.

## Optical characterization of the colloidal gold solution

UV–Vis spectroscopy can provide further insight into the synthesis of PNIPAM-stabilized gold nanoparticles by correlating the maximum position and the full width at half maximum (FWHM) of the absorption peak to the mean particle diameter, its monodispersity, and the interaction between metal nanoparticles. Figure 3a shows, for PGR 180:1 as an example, an increase in the intensity of the peak with each of the four growth steps. The insets show representative images of particles at the first ($\approx$4 nm) and last growth stages ($\approx$26 nm). Figure 3b shows that the increase in the area under the peak with each synthesis step is nearly independent of the PGR, i.e., that the polymer does not influence the number of particles formed and suggests that PNIPAM does not act as a strong nucleation agent, in contrast to the synthesis of silver (Morones and Frey 2007). The increase in area with growth cycles is approximately linear and shows little saturation.

Peak maxima vary little from 528 nm for lower PGRs, to 533 nm for higher PGRs, in agreement with the relatively constant particle diameter of $\sim$27 nm for all PGRs (Fig. 3c). The absorption peak, however, is redshifted by 7 nm relative to 26 nm-sized control particles grown with AsA from sodium citrate-synthesized seeds (Brown et al. 2000; Jain et al. 2006) The stabilization of gold nanoparticles with sodium citrate or AsA is due to surface charges, and the nanoparticle surfaces are therefore in direct contact with the environment so that as predicted by Mie theory, the LSPR maximum is further to the blue than when a polymer, such as PNIPAM, is attached to the surface (Xu et al. 2007). This also shows that the polymer is in intimate contact with the nanoparticle even in the hydrated state below the LCST.

The FWHM of the extinction peak depends on the PGR, but this dependence decreases with each synthesis step to less than 10 nm difference between the largest and smallest PGRs considered (Fig. 3d). The broadening of the peak at higher PGR is significant during the initial steps, indicating either very high size dispersion at high PGRs, or a spectral broadening due to the close proximity of small gold clusters. The latter is more likely, and would suggest the presence of several particles in one cocoon initially, so that their electromagnetic fields interact. The strong decrease in FWHM would then indicate Ostwald ripening and the formation of larger particles during the growth

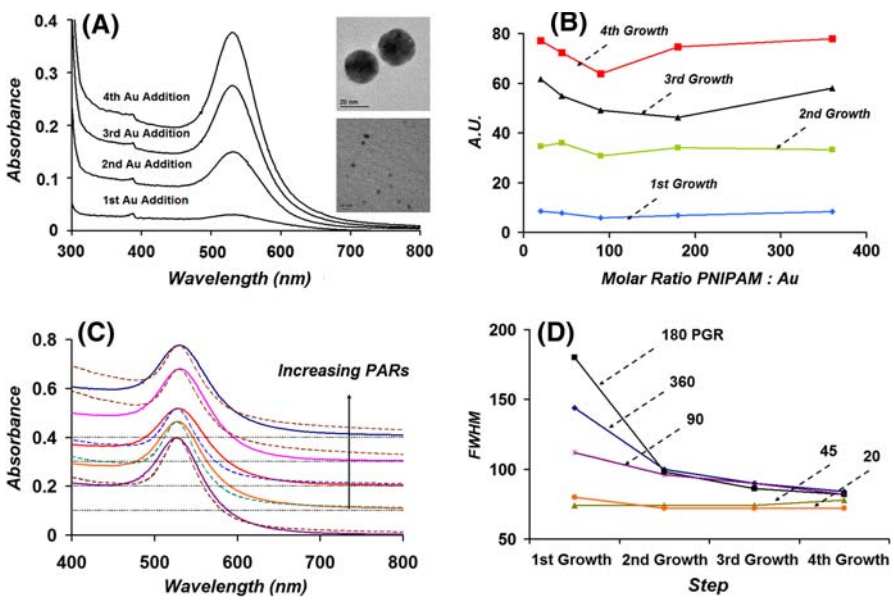


**Fig. 3** **a** Measured UV–Vis extinction spectra for the four reduction steps for the 360:1 PGR sample. *Top inset* is a TEM image that shows the spherical 27 nm particles at the last growth step. *Lower inset* shows the spherical particles at the initial step. **b** Area under the curve of the extinction spectra at each PGR. **c** Measured UV–Vis extinction spectra for the five PGRs shown in **b** (*offset* for clarity). **d** Full-width-at-half-maximum for the five PGRs as a function of the growth step

cycles, which is in agreement with the lack of a significant number of PNIPAM cocoons with multiple particles seen with TEM after four growth cycles. This explanation implies that the strong reduction in FWHM for the higher PGRs indicates that more nuclei are being formed initially and that PNIPAM can act as a nucleating agent. However, because the area under the peak did not depend on the PGR significantly (Fig. 3b), the nucleation activity is most likely not as strong as in the synthesis of PNIPAM–silver nanocomposites (Morones and Frey (2007)). The increase in peak intensity and the reduction of the FWHM with each growth stage also corroborates that the predominant phenomenon is uniform growth of the particles, since the reduction of the ionic gold takes place at the surface of the particle seeds (Brown et al. 2000; Jain et al. 2006; Jana et al. 2001b; Niu et al. 2007).

Mie model extinction spectra for spherical concentric shells are overlaid in Fig. 3c for the mean gold particle size distributions measured for each PGR. The PNIPAM shell refractive index and the layer thickness were fit parameters, but because the two parameters are not completely independent, a shell thickness of 33 nm in the hydrated state was assumed for consistency. This shell thickness was based on the expected volume of a random coil of the polymer in the hydrated state plus the metal particle volume to obtain a new radius of the combined particle. The Mie calculation, with a refractive index of 1.36 for the shell as seen for PNIPAM, (Harmon et al. 2003) reproduces the maximum position and the FWHM for PGRs of less than 90:1 quite well. PGRs of 180:1 and 360:1 had to be fitted with a refractive index of 1.39 to closely reproduce the maximum position. The measured spectra also have larger FWHM. A possible explanation is that the polymer shell is composed of a varying number of polymer chains, so that the cocoon thickness varies and produces some peak broadening. Alternatively, polymer cocoons could contain more than one metal nanoparticle, but this is unlikely because the TEM analysis did not show a significant number of such multiple particles.

## Thermal switching

The thermal response of the nanocomposite was studied in an optical microscope by recording the light transmittance when the temperature is increased (Fig. 4). Two capillaries, one containing a control sample (PNIPAM) and the other the nanocomposite (PNIPAM–Au, PGR 360:1, $3.2 \times 10^{15}$ gold particles/L solution), were placed side by side and heated uniformly, followed by passive cooling to room temperature. The thermal switching of both the control and the nanocomposite is fast and reversible with no fatigue. The polymer and the PNIPAM–gold particles, however, have different resolubilization times, with the PNIPAM–gold particle suspension requiring about twice as long as the pure polymer solution to become fully transparent after turning off the heat (Fig. 4a). This could be due to a difference in the adhesion strength in the aggregates forming above the LCST. More likely, however, smaller

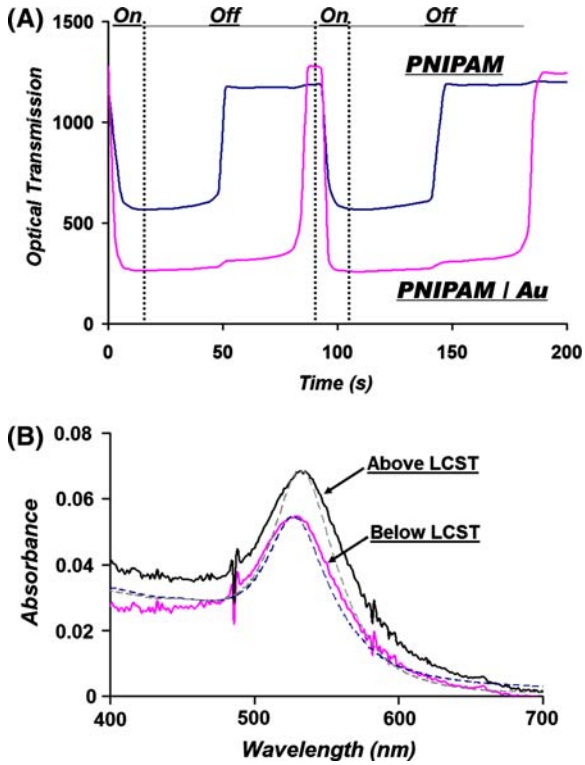


**Fig. 4** **a** Optical transmission of PNIPAM (*top*) and a colloidal PNIPAM–Au suspension (*bottom*) switched reversibly by increasing the temperature and allowing the sample to cool passively. On and off heating times are indicated. **b** UV–Vis extinction spectra for a very dilute sample of PGR 45:1. A ~6 nm peak shift in the extinction peak is induced by the precipitation of the nanoparticles. A theoretical Mie model spectrum is overlaid (*dashes*)

aggregates may still exist in both cases, but only PNIPAM–gold composites scatter visibly due to the much larger scattering cross section of the gold particles relative to a pure polymer coil, which then are undetectable. The small increase in transmission observed for the PNIPAM–gold particle suspension when the control becomes transparent is an artifact of the strong contrast changes at constant camera gain.

UV–Vis spectroscopy of very dilute samples showed the dependence of the extinction spectra on temperature and provided additional information about the local environment and the relative distance between the nanoparticles below and above the LCST. A small spectral redshift of 6 nm in the peak position is seen for all samples after heating the sample to above the LCST temperature, as shown in Fig. 4b for a PGR of 45:1. The spectra demonstrate two features: upon increasing the temperature to above the LCST, the FWHM remains unchanged, and the shift in peak position is small. Both features indicate that the gold nanoparticles mainly experience a change in their local environment due to the collapse of the surrounding polymer, and the influence due to electromagnetic interaction between metal particles is small, in agreement with results for silver (Morones and Frey (2007)), but opposite to grafted NIPAM-gold nanoparticles (Raula et al. 2003). A possible explanation of this discrepancy may be the different background compensation performed there for the spectrum. The extinction spectrum above the LCST can be fit well to a Mie concentric shell model using a shell thickness of 12 nm, based on the TEM images (Fig. 2), and a refractive index for the PNIPAM shell of 1.46 in the collapsed state (Harmon et al. 2003). This indicates that the PNIPAM–gold particles remain separate entities during the aggregation process, and that the interaction of the electromagnetic fields around the metal nanoparticles does not dominate.

## Optical switching

Switching the solubility of the PNIPAM–gold composite by varying the temperature can also be achieved indirectly through local heating of the metal nanoparticles by irradiation at the surface plasmon resonance wavelength. Figure 5a shows an optical switching cycle performed at a temperature of 31 °C, close to the LCST. Again, two capillaries were illuminated simultaneously, one with a control containing PNIPAM without gold, and one with a 360:1 PGR composite at $3.2 \times 10^{15}$ gold particles/L. Both capillaries were illuminated for 20 s at 800 mW/cm$^2$ followed by passive cooling. Only the composite shows a transition beginning quickly after 3 s and reaching high turbidity at $\sim$15 s. The behavior of the nanocomposite to thermal and optical stimulation is similar. However, there is a small delay after the start of the light exposure due to efficient heat conduction of the nonabsorbent environment, which also makes

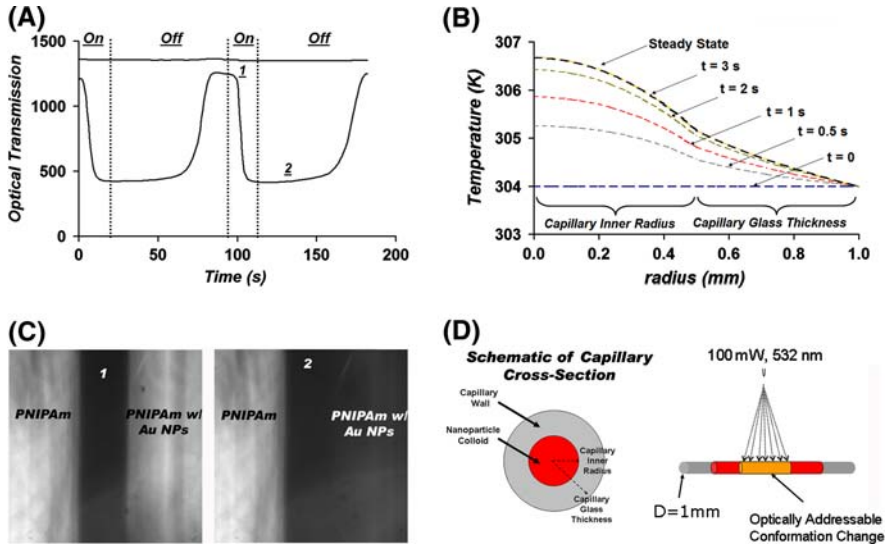


**Fig. 5** **a** Optical transmission of PNIPAM (*top curve*) and a colloidal PNIPAM–Au suspension (*bottom curve*) switched reversibly by exposure to 532 nm laser light. On and off exposure times are indicated by dotted lines. **b** Transient and steady-state temperature profiles calculated for the cylindrical capillary. **c** Optical microscopy image of the PNIPAM and the PNIPAM–Au composite at positions 1 and 2 indicated in (**a**). **d** Experimental setup in top (*left*) and side view (*right*)

the resuspension time shorter than for thermal heating. This indicates that the temperature increase is much smaller for optical than for thermal heating, and the aggregates are therefore presumably smaller.

Different than gold nanoparticles dispersed in a gel, each PNIPAM–gold composite builds an optical switch of its own that acts due to a change in hydration, although turbidity measurements rely on the aggregation of several particles into larger clusters. We compared the analytically calculated steady state and the numerically determined generation of the temperature distribution and found that the time-dependant heat generation and temperature profiles in the colloid reach the analytically determined steady state after $\sim$3 s, which agrees with the experiments. Despite the large heat conductance of the aqueous environment and the glass, the heat generated by a relatively low-power laser is sufficient for switching the polymer conformation. At steady state, the calculated temperature difference is $\sim$2.5 °C between the environment (air) and the center of the colloidal suspension, which is a reasonable temperature increase to explain the experimental results.

The mechanism of optical conformational switching of the PNIPAM–gold composite relies on the energy conversion of the optical energy absorbed by the gold nanoparticles at the surface plasmon resonance, which is energetically lower than the lowest interband transition of gold at around 470 nm. The LSPR energy absorbed in the nanoparticles is dissipated as heat to the surrounding thermally sensitive PNIPAM. The heat generated by individual nanoparticles and clusters irradiated by light at the LSPR wavelength has been measured by embedding the nanoparticles in ice and measuring the rate and volume of melting ice surrounding the particles (Richardson et al. 2006). Others have estimated the heat from a single gold particle by measuring the heat conduction of core-shell nanoparticles immersed in different media, such as water (Ge et al. 2004) and polystyrene (Ge et al. 2005), or by quantifying the quenching of fluorescence in a microfluidic channel (Liu et al. 2005). Gold nanoparticles embedded in ice at particle concentrations, three orders of magnitude lower than in our experiments were used to measure the total ice volume melting in the focus of a laser beam (Richardson et al. 2006). The heat to melt the ice was generated under conditions of four times the heat conductivity compared to liquid water and two orders of magnitude higher power density than used in our experiments. The heat generated by gold nanocrescents in a partially filled microfluidic channel near the air-water interface was estimated using temperature-dependent fluorescence quenching to induce a temperature increase of at least 60 °C, and was sufficient to cause water evaporation (Liu et al. 2005). These high heating rates were achieved in a thermally insulated environment of a microfluidic channel at an air–water interface with a focused laser at a power density one order of magnitude larger and a particle concentration of about one quarter compared to our case. Still, all three findings are consistent with our experimental results and the estimates for the heat that can be generated.

The nanocomposite optical response is faster, in both directions, than reported for responsive hydrogels (Jones and Lyon 2003; Sershen et al. 2005; Sershen et al. 2002). Smaller hydrogels have shown faster response times, although high-power lasers are still necessary (Shiotani et al. 2007). To the best of our knowledge, this is the first time that the optical switching of single PNIPAM chains using indirect heating from gold nanoparticles has been reported. Optical switching of PNIPAM using organic groups, such as spirobenzene (Szilagyi et al. 2007), spiropyrane (Nayak et al. 2006), and azobenzene (Brinker 2004) is far slower, even for free polymer chains. In contrast, experiments with gold nanoparticles in ice (Richardson et al. 2006) and single core-shell particles (Ge et al. 2005) showed very fast thermal equilibration—on the order of picoseconds—between the particles and their environments.

The time-dependent dissipation of heat from a single particle has recently been calculated analytically, assuming a constant temperature and finite heat capacity across the particle and no interfacial heat resistance (Oliver 2008). This time-dependent model applied to the experimental conditions used here with an unfocused 100 mW laser shows that steady-state conditions around a single particle are reached within microseconds. At steady state, the temperature increase at the surface of the particle is $\Delta T = 1/3\, Qa^2/\kappa_w$, with $\kappa_w$ the heat conductivity of water, $a$, the particle radius, and $Q$, the heat density. This is consistent with other results (Ge et al. 2004, 2005; Liu et al. 2005), and indicates that the aggregation process is the rate-limiting step in the turbidity experiments.

The generated temperature change for the given experimental conditions decreases less than linearly with decreasing particle number, and we estimate that a temperature increase of greater than 1 °C can be achieved locally in a homogeneous and thermally conducting medium under conditions, similar to those used in the experiments described above with a laser beam focused to about 100 μm. In fact, we have been able to locally precipitate the PNIPAM–gold particles within a spot inside the capillary under conditions as described above, but using a focused laser beam, and we achieved very fast switching in both directions (results not shown). The irradiated volume contained on the order of 3 attomoles of particles. By increasing the laser power and reducing the focus, we estimate that even under thermally conducting conditions, such as in a homogeneous water bath, irradiation of a few hundred gold particles could induce a significant temperature increase that would allow for experimentally achievable switching conditions.

## Conclusions

We have shown for the first time that AsA can be used to nucleate and grow gold nanoparticles at room temperature in a simple one-pot synthesis using PNIPAM as the capping agent to form a stable and opto-thermally responsive PNIPAM–Au nanocomposite. This is possible even though PNIPAM has a weaker interaction with gold than with other metals, such as silver. This weaker interaction may explain why PNIPAM is important in the nucleation process, but, in contrast to silver, the number of particles appears to be independent of the amount of polymer present. PNIPAM controls the gold nanoparticle size to within a standard deviation of ~22% for higher PGRs (360 and 180), which is comparable to sodium citrate reduction and to sodium-borohydrate reduction to create seeds and subsequent ascorbic acid reduction. At lower PGRs, the size control is weaker and the standard deviation increases to 35%. The synthesis achieves relatively large gold nanoparticles compared to thiol- or thioester-stabilized gold nanoparticle synthesis, which allows for a more efficient light harvest.

We have shown that the particles can be reversibly aggregated and resuspended with fast response times—on the order of seconds—by heat and light at the LSPR wavelength (532 nm). Stability of the particles is achieved through cocoon-like structures of PNIPAM–Au. The optical properties indicate the change in the polymer state due to temperature, which changes the LSPR peak position by ~6 nm above the LCST, indicating that the cocoons still separate each particle in the aggregate.

We compared our experimental results with heat conduction models that describe the optical switching of the nanocomposite colloidal suspension. The model predicts a 2.5 °C temperature increase for the experimental setup used here, which agrees with our experimental results. By optimizing particle size and laser power density, the number of particles could be significantly reduced even under thermally conducting experimental conditions. We also estimated the switching time to be on the order of microseconds, much faster than can be achieved with gels or dyes, and even turbidity measurements show switching within a few seconds. The PNIPAM–gold nanocomposites, therefore, build an optically triggered nanoactuator that can be used as a switch for biotechnological applications through changes in the hydration. Improving the conversion of light to heat through a controlled nonspherical particle shape with a PNIPAM shell could increase the switching efficiency significantly (Kou et al. 2007).

## Experimental

### Materials

Deionized water with a resistivity of at least (18.0 MΩ cm) (EPure, Barnstead Thermolyne) was used in all experiments. *N*-Isopropyl acrylamide (NIPAM) (Fisher Scientific) was recrystallized once in hexane (Fisher Scientific) and stored at −20 °C until use. Ascorbic acid (AsA) (Fisher Scientific), hydrogen tetrachloroaureate (III) hydrate ($HAuCl_4$), *N*,*N*,*N*′,*N*′-tetramethyl ethylene diamine (TEMED), and ammonium persulfate (APS) (all Sigma Aldrich) were used as purchased.

### Polymer synthesis

PNIPAM was synthesized by free-radical polymerization of NIPAM using the APS and TEMED redox initiator system. Nitrogen is bubbled through an aqueous NIPAM solution (200 mL, 0.3 M) for

20 min and then sealed under a nitrogen atmosphere during reaction. The polymerization is started by the addition of each of the redox system components (1% wt each), and left to proceed for 2 h. The aqueous PNIPAM product is poured into four times the volume of ethanol for precipitation—at that mixture PNIPAM is insoluble (Hirotsu et al. 1995), followed by centrifugation at 16,600*g* for 15 min, and resuspension in water. This procedure is repeated three times in order to remove any unreacted monomer or initiator from the solution. The aqueous polymer solution is freeze dried and stored at −20 °C in powder form until further use. Gel permeation chromatography (GPC) determined the mass average molecular weight of the polymer used in these experiments to be MW = 516,000 with a polydispersity index of 2.54. GPC experiments were performed using dimethylformamide (DMF) as an eluent in a Waters 515 HPLC solvent pump and two PLgel mixed-C columns (5 μm bead size for MW range 200–2000,000 g/mol) (Polymer Laboratories, Inc.)

## Preparation of Au–PNIPAM colloids

Aqueous mixtures of $HAuCl_4$ (0.1 mmol) and PNIPAM at four different polymer to gold ratios (PGR) (20, 45, 180, and 360 times the molar amount of repeat units of PNIPAM relative to ionic gold ions) were prepared and stirred at room temperature. After 5 min of stirring, AsA is added to achieve a total volume of (5 mL of a 3:1 molar ratio of AsA/$Au^{+3}$), and stirred for an additional 10 min. This initial process is followed by repeated (three times) addition of $HAuCl_4$ solution (200 μL, 0.01 m) followed by an equimolar amount of AsA in 10 min intervals. Once the growth has terminated, the solution is heated to 35 °C during centrifugation at 16,600*g* for 15 min inducing the precipitation of first the Au–PNIPAM and then the polymer. The supernatant is discarded and the precipitate resuspended in water. Finally, the mixture of PNIPAM and Au–PNIPAM composite is centrifuged at 20 °C and 25,700*g* for 10 min, discarding the PNIPAM supernatant, and followed by re-suspending the nanoparticles in water; this process is performed twice.

## Transmission electron microscopy

Transmission electron microscopy (TEM) images were obtained with a JEOL 2010-F at an acceleration voltage of 200 kV. The specimens were prepared by placing a drop of aqueous colloidal suspension onto a carbon-coated copper grid, incubating for 30 min, and then aspirating excess solvent with filter paper. Shape and size distributions were determined from enlarged photographs of the TEM images using at least 200 particles for each sample. For negative staining, a uranyl acetate aqueous solution (0.1% w/v) was placed on a piece of parafilm, and a TEM grid, prepared as described above, was placed on top of the drop for 1 min. Afterwards, the sample was aspirated using filter paper and left to dry overnight. The sample was then analyzed as described above.

## UV–Visible spectroscopy

The LCST of PNIPAM alone and the spectral properties of PNIPAM–Au colloids in aqueous solution were measured using a temperature-controlled CARY 5000 UV–Vis spectrophotometer. When needed, the temperature was raised from 25 to 36 °C at a rate of 1 °C/min. Recorded spectra were analyzed for peak position and peak width of the LSPR resonance. UV–Vis spectroscopy to compare spectra below and above the LCST was performed with very dilute samples to minimize the scattering of large aggregates above the LCST.

## Thermal and optical switching experiments

The thermal and optical responses of the PNIPAM–Au nanocomposites were studied using colloidal samples with an estimated $3.164 \times 10^{15}$ gold particles/L, assuming complete reduction of the gold ions during the synthesis, and a particle radius of 13 nm consistent with our experimental results. The total gold ion concentration after four growth steps was (1.3 mmol), which can be converted into a particle concentration using the molecular weight of metallic gold (197 g/mol) and the metallic gold density (19.32 g/$cm^3$). The concentration determined this way is an upper limit assuming all gold is converted to nanoparticles. These concentrations agree, however, within a factor of two with those determined from extinction measurements using a linear dependence of the logarithm of the molar extinction coefficient with the logarithm of the nanoparticle diameter (Liu et al. 2007). Small droplets of PNIPAM–Au colloids and a PNIPAM control where

sealed in two glass capillaries by melting the ends on both sides. The capillaries were placed side by side, and then they were uniformly heated for 20 s, until reaching a temperature above the LCST. Followed, the sample was left at room temperature to undergo passive cooling under the optical microscope. The light transmittance was recorded for at least two complete heat–cool cycles. The optical switching experiments were performed in a similar way with the microscope environment held at 31 °C. Both capillaries were irradiated for periods of 20 s with a 100 mW 532 nm diode-pumped laser with a beam diameter of $\sim$4 mm. For the thermal and optical switching, the capillaries were imaged with time-lapse microscopy and grayscale information was extracted from the image sequence using ImageJ (NIH).

## Modeling

Mie theory for spherical concentric core shell particles was used to model the experimental extinction spectra. The model was adapted from the code in (Bohren and Huffman 1998) and written in IGOR Pro (Wavemetrics), using the refractive index for gold from reference (Johnson and Christy 1972). Modeling of the heat profiles was performed by solving the steady state Fourier heat transfer equations analytically and the non-steady state equations numerically using the Finite Element Method (FEMLAB, COMSOL Multiphysics 3.3). A homogenous dispersion of uniformly heated colloidal particles was assumed for a concentric cylinder geometry as used in the experiment, a glass capillary with inner and outer diameters of $R_1 = 0.5$ mm and $R_2 = 1$ mm, respectively (see Fig. 5d).

**Acknowledgments** The authors thank Dr. N. A. Peppas for helpful discussion. The work was supported in part by a grant from the Welch Foundation (F-1574), and by support through the Center for Nano and Molecular Science and Technology at UT Austin. Jose Ruben Morones would also like to acknowledge funding from the Consejo Nacional de Ciencia y Tecnologia (CONACyT) in Mexico.

## References

Andreescu D, Sau TK, Goia DV (2006) Stabilizer-free nanosized gold sols. J Colloid Interface Sci 298:742–751

Ballauff M, Lu Y (2007) "Smart" nanoparticles: preparation, characterization and applications. Polymer 48:1815–1823

Beebe DJ, Moore JS, Bauer JM, Yu Q, Liu RH, Devadoss C, Jo BH (2000) Functional hydrogel structures for autonomous flow control inside microfluidic channels. Nature 404:588–590

Ben-Moshe M, Alexeev VL, Asher SA (2006) Fast responsive crystalline colloidal array photonic crystal glucose sensors. Anal Chem 78:5149–5157

Bohren CF, Huffman DR (1998) Absorption and scattering of light by small particles. Wiley-VCH, New York

Brinker CJ (2004) Evaporation-induced self assembly: functional nanostructures made easy. MRS Bull 29:631–640

Brown KR, Walter DG, Natan MJ (2000) Seeding of colloidal Au nanoparticle solutions. 2. Improved control of particle size and shape. Chem Mater 12:306–313

Brust M, Walker M, Bethell D, Schiffrin DJ, Whyman R (1994) Synthesis of thiol-derivatized gold nanoparticles in a 2-phase liquid-liquid system. J Chem Soc Chem Commun 80:1–802

Brust M, Fink J, Bethell D, Schiffrin DJ, Kiely C (1995) Synthesis and reactions of functionalised gold nanoparticles. J Chem Soc Chem Commun 1655–1656

Byrne ME, Park K, Peppas NA (2002) Molecular imprinting within hydrogels. Adv Drug Deliv Rev 54:149–161

Calvert P (2008) Gel sensors and actuators. MRS Bull 33:207–212

Chen C-W, Akashi M (1997) Preparation of ultrafine platinum particles protected by poly(nisopropylacrylamide) and their catalytic activity in the hydrogenation of allyl alcohol. J Polym Sci A 35:1329–1332

Chen C-W, Chen M-Q, Serizawa T, Akashi M (1998) In situ formation of silver nanoparticles on poly(n-isopropylacrylamide)-coated polystyrene microspheres. Adv Mater 14:1122–1126

Chen C-W, Serizawa T, Akashi M (2002) In situ formation of Au/Pt bimetallic colloids on polystyrene microspheres: control of particle growth and morphology. Chem Mater 14:2232–2239

Dai S, Ravi P, Tam KC (2008) pH-Responsive polymers: synthesis, properties and applications. Soft Matter 4:435–449

Edahiro J, Sumaru K, Tada Y, Ohi K, Takagi T, Kameda M, Shinbo T, Kanamori T, Yoshimi Y (2005) In situ control of cell adhesion using photoresponsive culture surface. Biomacromolecules 6:970–974

Eddington DT, Beebe DJ (2004) Flow control with hydrogels. Adv Drug Deliv Rev 56:199–210

Frens G (1973) Controlled nucleation for regulation of the particle size in monodisperse gold solutions. Nat Phys Sci 241:20–22

Frey W, Meyer DE, Chilkoti A (2003a) Dynamic addressing of a surface pattern by a stimuli-responsive fusion protein. Adv Mater 15:248–251

Frey W, Meyer DE, Chilkoti A (2003b) Thermodynamically reversible addressing of a stimuli responsive fusion protein onto a patterned surface template. Langmuir 19:1641–1653

Garcia A, Marquez M, Cai T, Rosario R, Hu ZB, Gust D, Hayes M, Vail SA, Park CD (2007) Photo-, thermally, and pH-responsive microgels. Langmuir 23:224–229

Ge Z, Cahill DG, Braun PV (2004) AuPd metal nanoparticles as probes of nanoscale thermal transport in aqueous solution. J Phys Chem B 108:18870–18875

Ge Z, Kang Y, Taton TA, Braun PV, Cahill DG (2005) Thermal transport in Au-core polymer-shell nanoparticles. Nano Lett 5:531–535

Gil ES, Hudson SM (2004) Stimuli-reponsive polymers and their bioconjugates. Prog Polym Sci 29:1173–1222

Goia DV, Matijevic E (1998) Preparation of monodispersed metal particles. New J Chem 19:1203–1215

Goia DV, Matijevic E (1999) Tailoring the particle size of monodispersed colloidal gold. Colloids Surf Physicochem Eng Asp 146:139–152

Halas N (2005) Playing with plasmons: tuning the optical resonant properties of metallic nanoshells. MRS Bull 30:362–367

Harmon ME, Kuckling D, Frank CW (2003) Photo-cross-linkable PNIPAAm copolymers. 2. Effects of constraint on temperature and pH-responsive hydrogel layers. Macromolecules 36:162–172

Higuchi A, Hamamura A, Shindo Y, Kitamura H, Yoon BO, Mori T, Uyama T, Umezawa A (2004) Photon-modulated changes of cell attachments on poly(spiropyran-co-methyl methacrylate) membranes. Biomacromolecules 5:1770–1774

Hilt JZ, Byrne ME, Peppas NA (2006) Microfabrication of intelligent biomimetic networks for recognition of D-glucose. Chem Mater 18:5869–5875

Hirotsu S, Okajima T, Yamamoto T (1995) Anomalous aggregation pattern observed on gels in mixed-solvent. Macromolecules 28:775–777

Hoffman AS, Stayton PS (2004) Bioconjugates of smart polymers and proteins: synthesis and applications. Macromol Symp 207:139–151

Hugel T, Holland NB, Cattani A, Moroder L, Seitz M, Gaub HE (2002) Single-molecule optomechanical cycle. Science 296:1103–1106

Hutter E, Fendler JH (2004) Exploitation of localized surface plasmon resonance. Adv Mater 16:1685–1706

Irie M, Kungwatchakun D (1992) Stimuli-responsive polymers—photostimulated reversible phase-separation of aqueous-solutions of poly(N-isopropylacrylamide) with pendant azobenzene groups. Proc Jpn Acad B 68:127–132

Jager EWH, Smela E, Inganas O (2000) Microfabricating conjugated polymer actuators. Science 290:1540–1545

Jain PK, Lee KS, El-Sayed IH, El-Sayed MA (2006) Calculated absorption and scattering properties of gold nanoparticles of different size, shape, and composition: applications in biological imaging and biomedicine. J Phys Chem B 110:7238–7248

Jana NR, Gearheart L, Murphy CJ (2001a) Evidence for seed-mediated nucleation in the chemical reduction of gold salts to gold nanoparticles. Chem Mater 13:2313–2322

Jana NR, Gearheart L, Murphy CJ (2001b) Seeding growth for size control of 5–40 nm diameter gold nanoparticles. Langmuir 17:6782–6786

Jiang H, Kelch S, Lendlein A (2006) Polymers move in response to light. Adv Mater 18:1471–1475

Johnson PB, Christy RW (1972) Optical constants of the noble metals. Phys Rev B 6:4370–4379

Jones CD, Lyon AL (2003) Photothermal patterning of microgel/gold nanoparticle composite colloidal crystals. J Am Chem Soc 125:460–465

Juodkazis S, Mukai N, Wakaki R, Yamaguchi A, Matsuo S, Misawa H (2000) Reversible phase transitions in polymer gels induced by radiation forces. Nature 408:178–181

Kaholek M, Lee W-K, LaMattina B, Caster KC, Zauscher S (2004) Fabrication of stimulus-responsive nanopatterned polymer brushes by scanning-probe lithography. Nano Lett 4:373–376

Kim J-H, Lee TR (2007) Hydrogel-templated growth of large gold nanoparticles: synthesis of thermally responsive hydrogel-nanoparticle composites. Langmuir 23:6504–6509

Kim DJ, Kang SM, Kong B, Kim W-J, Paik H-J, Choi H, Choi IS (2005) Formation of thermoresponsive gold nanoparticle/PNIPAAm hybrids by surface-initiated, atom transfer radical polymerization in aqueous media. Macromol Chem Phys 206:1941–1946

Kimling J, Maier M, Okenve B, Kotaidis V, Ballot H, Plech A (2006) Turkevich method for gold nanoparticle synthesis revisited. J Phys Chem B 110:15700–15707

Kou X, Ni W, Tsung C-K, Chan K, Lin H-Q, Stucky GD, Wang J (2007) Growth of gold bipyramids with improved yield and their curvature-directed oxidation. Small 3:2103–2113

Kungwatchakun D, Irie M (1988) Photoresponsive polymers. Photocontrol of the phase separation temperature of aqueous solutions of poly[N-isopropylacrylamide-co-N-(4-phenylazophenyl)]acrylamide. Makromol Chem Rapid Comm 9:243–246

Lahann J, Langer R (2005) Smart materials with dynamically controllable surfaces. MRS Bull 30:185–188

Langer R, Tirrell DA (2004) Designing materials for biology and medicine. Nature 428:487–492

Liu J, Lu Y (2006) Smart nanomaterials responsive to multiple chemical stimuli with controllable cooperativity. Adv Mater 18:1667–1671

Liu GL, Kim J, Lu Y, Lee LP (2005) Optofluidic control using photothermal nanoparticles. Nat Mater 10:1–6

Liu X, Atwater M, Wang J, Huo Q (2007) Extinction coefficient of gold nanoparticles with different sizes and different capping ligands. Colloids Surf B 58:3–7

Liz-Marzan LM (2006) Tailoring surface plasmons through the morphology and assembly of metal nanoparticles. Langmuir 22:32–41

Morones J, Frey W (2007) Environmentally sensitive silver nanoparticles of controlled size synthesized with PNIPAM as a nucleating and capping agent. Langmuir 23:8180–8186

Nath N, Chilkoti A (2001) Interfacial phase transition of an environmentally responsive elastin biopolymer adsorbed on functionalized gold nanoparticles studied by colloidal surface plasmon resonance. J Am Chem Soc 123:8197–8202

Nayak S, Lyon LA (2004) Photoinduced phase transitions in poly(N-isopropylacrylamide) microgels. Chem Mater 16:2623–2627

Nayak A, Liu H, Belfort G (2006) An optically reversible switching membrane surface. Angew Chem Int Ed Engl 45:4094–4098

Niu J, Zhu T, Liu Z (2007) One-step seed-mediated growth of 30–150 nm quasispherical gold nanoparticles with 2-mercaptosuccinic acid as a new reducing agent. Nanotechnology 18:325607

Nuss S, Bottcher H, Wurm H, Hallensleben ML (2001) Gold nanoparticles with covalently attached polymer chains. Angew Chem Int Ed Engl 40:4016–4018

O'Neal DP, Hirsch LR, Halas NJ, Payne JD, West JL (2004) Photo-thermal tumor ablation in mice using near infrared-absorbing nanoparticles. Cancer Lett 209:171–176

Ohno K, Koh K, Tsujii Y, Fukuda T (2002) Synthesis of gold nanoparticles coated with well-defined, high-density polymer brushes by surface-initiated living radical polymerization. Macromolecules 35:8989–8993

Oliver DL (2008) Analytical solution for heat conduction near an encapsulated sphere with heat generation. J Heat Transf 130:024502

Owens DE, Eby JK, Jian Y, Peppas NA (2007) Temperature-responsive polymer-gold nanocomposites as intelligent therapeutic systems. J Biomed Mater Res A 83A:692–695

Peppas NA, Khare AR (1993) Preparation, structure and diffusional behavior of hydrogels in controlled release. Adv Drug Deliv Rev 11:1–35

Peppas NA, Hilt JZ, Khademhosseini A, Langer R (2006) Hydrogels in biology and medicine: from molecular principles to bionanotechnology. Adv Mater 18:1345–1360

Pong FY, Lee M, Bell JR, Flynn NT (2006) Thermoresponsive behavior of poly(N-isopropylacrylamide) hydrogels containing gold nanostructures. Langmuir 22:3851–3857

Pyun J, Kowalewski T, Matyjaszewski K (2003) Synthesis of polymer brushes using atom transfer radical polymerization. Macromol Rapid Commun 24:1043–1059

Radt B, Smith TA, Caruso F (2004) Optically addressable nanostructured capsules. Adv Mater 16:2184–2189

Raula J, Shan J, Nuopponen M, Niskanen A, Jiang H, Kauppinen EI, Tenhu H (2003) Synthesis of gold nanoparticles grafted with a thermoresponsive polymer by surface-induced reversible-addition-fragmentation chain-transfer polymerization. Langmuir 19:3499–3504

Richardson HH, Hickman ZN, Govorov AO, Thomas AC, Zhang W, Kordesch ME (2006) Thermooptical properties of gold nanoparticles embedded in ice: characterization of heat generation and melting. Nano Lett 6:783–788

Schild HG (1992) Poly (N-Isopropylacrylamide)—experiment, theory and application. Prog Polym Sci 17:163–249

Sershen SR, Westcott SL, Halas NJ, West JL (2000) Temperature-sensitive polymer-nanoshell composites for photothermally modulated drug delivery. J Biomed Mater Res 51:293–298

Sershen SR, Westcott SL, West JL, Halas NJ (2001) An opto-mechanical nanoshell-polymer composite. Appl Phys B 73:379–381

Sershen SR, Westcott SL, Halas NJ, West JL (2002) Independent optically addressable nanoparticle-polymer optomechanical composites. Appl Phys Lett 80:4609

Sershen SR, Mensing GA, Ng M, Halas NJ, Beebe DJ, West JL (2005) Independent optical control of microfluidic valves formed from optomechanically responsive nanocomposite hydrogels. Adv Mater 17:1366–1368

Shan J, Nuopponen M, Jiang H, Kauppinen E, Tenhu H (2003) Preparation of poly(N-isopropylacrylamide)-monolayer-protected gold clusters: synthesis methods, core size, and thickness of monolayer. Macromolecules 36:4526–4533

Shan J, Nuopponen M, Jiang H, Viitala T, Kauppinen E, Kontturi K, Tenhu H (2005) Amphiphilic gold nanoparticles grafted with poly(N-isopropylacrylamide) and polystyrene. Macromolecules 38:2918–2926

Shimoboji T, Larenas E, Fowler T, Kulkarni S, Hoffman AS, Stayton PS (2002) Photoresponsive polymer-enzyme switches. Proc Natl Acad Sci USA 99:16592–16596

Shiotani A, Mori T, Niidome T, Niidome Y, Katayama Y (2007) Stable incorporation of gold nanorods into N-isopropylacrylamide hydrogels and their rapid shrinkage induced by near-infrared laser irradiation. Langmuir 23:4012–4018

Shoenfeld NA, Grodzinsky AJ (1980) Contribution of electrodiffusion to the dynamics of electrically stimulated changes in mechanical-properties of collagen membranes. Biopolymers 19:241–262

Slocik JM, Tam F, Halas NJ, Naik RR (2007) Peptide-assembled optically responsive nanoparticle complexes. Nano Lett 7:1054–1058

Strzegowski LA, Martinez MB, Gowda DC, Urry DW, Tirrell DA (1994) Photomodulation of the inverse temperature transition of a modified elastin poly(pentapeptide). J Am Chem Soc 116:813–814

Szilagyi A, Sumaru K, Sugiura S, Takagi T, Shinbo T, Zrinyi M, Kanamori T (2007) Rewritable microrelief formation on photoresponsive hydrogel layers. Chem Mater 19:2730–2732

Wang CN, Flynn T, Langer R (2004) Controlled structure and properties of thermoresponsive nanoparticle-hydrogel composites. Adv Mate. 16:1074–1079

Xu H, Xu J, Jiang X, Zhu Z, Rao J, Yin J, Wu T, Liu H, Liu S (2007) Thermosensitive unimolecular micelles surface-decorated with gold nanoparticles of tunable spatial distribution. Chem Mater 19:2489–2494

Yousaf MN, Houseman BT, Mrksich M (2001) Using electroactive substrates to pattern the attachment of two different cell populations. Proc Natl Acad Sci USA 98:5992–5996

Zhao M, Crooks RM (1999) Intradendrimer exchange of metal nanoparticles. Chem Mater 11:3379–3385

Zheng P, Jiang X, Zhang X, Zhang W, Shi L (2006) Formation of gold@polymer Core-shell particles and gold particle clusters on a template of thermoresponsive and pH-responsive coordination triblock copolymer. Langmuir 22:9393–9396

Zheng J, Xu C, Hirai T (2008) Electromechanical nonionic gels. New J Phys 10:023016

Zhu M-Q, Wang L-Q, Exarhos GJ, Li ADQ (2004) Thermosensitive gold nanoparticles. J Am Chem Soc 126:2656–2657

Zhu LY, Wu WW, Zhu MQ, Han JJ, Hurst JK, Li ADQ (2007) Reversibly photoswitchable dual-color fluorescent nanoparticles as new tools for live-cell imaging. J Am Chem Soc 129:3524–3526